PAPER • **OPEN ACCESS**

Combustion Efficiency of Carbon-neutral Fuel using Micro-Combustor Designed for Aerospace Applications

To cite this article: M.G. De Giorgi *et al* 2024 *J. Phys.: Conf. Ser.* **2716** 012091

Combustion Efficiency of Carbon-neutral Fuel using Micro-Combustor Designed for Aerospace Applications

M.G. De Giorgi [1*], G. Cinieri [1], G. Marseglia [1], Z. Ali Shah [1], Ghazanfar Mehdi[1]

[1] University of Salento, Dep. Engineering for Innovation, Via per Monteroni, 73100 Lecce, Italy

***mariagrazia.degiorgi@unisalento.it**

Abstract. Recent advancements in the field of micro combustor research are growing for achieving high-performance systems in micro power generation and microelectromechanical devices. To mitigate the hazardous emissions from carbon fuels, as an alternative, zero-carbon-free fuels ammonia, and hydrogen are being explored in micro combustion processes. The distinctive feature of a micro combustor lies in its significantly higher area to volume ratio in comparison with traditional combustion systems, leading to accelerated combustion reaction rates. However, the small size of micro combustors poses a challenge in achieving efficient mixing of highly reactive fuels like hydrogen and ammonia with oxidizers. The unique properties of micro combustors can lead to differences in the combustion behavior of hydrogen and ammonia compared to larger-scale combustion systems. Hence, examining the performance of carbon-free fuels in micro combustors is crucial for the advancement of clean energy combustion systems. A numerical investigation on a Y-shaped micro-combustor was carried out to identify the aspects of non-premixed combustion of ammonia/air and hydrogen/air. The findings reveal that in the case of hydrogen combustion, stable flames were reached, even at low equivalence ratios. Therefore, the distinct combustion properties of hydrogen and ammonia result in varying NO_x emissions, with hydrogen generally leading to higher NO_x levels due to its higher flame temperature and increased thermal NO_x production.

1. Introduction

During the last three decades, combustion-based micro devices have revolutionized the field of energy conversion, thanks to their notable attributes such as low weight, high energy density, small dimensions, and extended lifespan [1]. The Sustainable Development Goals (SDGs) aimed for accomplishment by the year 2030 underscore the significance of enhancing the performance of micro thermal energy conversion systems. These systems not only provide energy advantages in addition, carry noteworthy impacts for both the economic and social aspects. Micro combustors play a pivotal role as key elements in streamlined energy systems, including micro-thermoelectric and micro-thermophotovoltaic systems [2], [3]. The length scale for micro-scale power generation devices is typically characterized as being below 1 mm [4]. The revolution in micro combustion technology has resulted in systems that are lighter, smaller, and possess higher energy density [5], [6]. To maintain a stable flame in micro burners proves to be challenging due to the high area to volume ratio and small residence time [7], [8]. The influence of geometry on micro combustion systems is currently the most relevant research topic. Changes in micro combustor geometry can significantly impact thermos-physical properties, including heat transfer rates and residence, thereby modifying device performance. As an example, Peng et al. performed numerical analysis to investigate the impacts of reducing wall thickness in hydrogen-air combustion with the aim of enhancing wall temperature and flame area [9]. Another crucial aspect that has gained recent attention is the examination of the influence of heightened thermal conductivity of the combustion area, as conferred in the literature. [10]. While hydrogen offers various advantages, challenges persist in terms of its storage, distribution, and the required infrastructure. One possible alternative fuel to hydrogen is ammonia. Ammonia, as a carbon-free fuel, has

obtained increasing interest as a pivotal candidate for future fuels, playing a significant role in the shift towards renewable energy sources. Several applications for ammonia as a future fuel have been suggested, spanning heavy transportation, clean power generation and energy storage [11]. Ammonia exhibits a low chemical reactivity which results lower flame speed compared to other conventional fuels. Consequently, achieving optimal combustion conditions for ammonia becomes challenging, particularly in micro combustors. This study contrasts the flame behavior of non-premixed mixtures of hydrogen-air and ammonia/air in a Y-shaped micro combustor that was previously experimentally tested by Xiang et al. [12], [13]. The impact of utilizing NH_3/air mixtures is discussed, considering emission reduction and combustion competence in comparison to the hydrogen condition. A CHEMKIN numerical model is developed and validated considering laminar burning velocity. In the second phase, the chemical equations scheme developed in CHEMKIN, encompassing all the particles generated during combustion, is transferred to steady-state CFD model using a continuum Navier–Stokes method. The model's validity is affirmed through a comparison of simulation results with experimental data. The numerical analyses are conducted using Ansys Fluent 2023 R2 [14]. The primary goal of this investigation is to examine the impact of H_2 and NH_3 on thermal performance and the environmental impact underlining the impacts of carbon-free fuels on a microscale path. Improved kinetic mechanisms have been implemented and validated for both NH_3/air and H_2/air mixture and validated by showing the comparison of predicted values laminar burning velocity with experimental data using CHEMKIN software. Employing a numerical CFD method, the paper advances beyond current understanding of thermo-chemical processes in micro combustors based on modern technology. It explores essential characteristics closely linked to the inefficiencies in heat exchange during the energy conversion systems.

2. Methodology

2.1 The geometric model of the micro-combustor

A detailed exploration is conducted on a specific 3D model geometry, which includes a Y-shaped micro combustor measuring length of 200mm, featuring an angle of 90-degree. The model incorporates two different inlet channels for respective fuels under consideration, namely hydrogen and ammonia, along with dry air. For more details see Xiang et al. geometry description [12], [13] .
The combustion chamber in this study is constructed with walls made of quartz glass, with the operating conditions set at a pressure of 1 atmosphere and a temperature of 300K. A symmetry plane boundary condition is applied to half geometry and discretization.

2.2 Combustion modelling and details of kinetic mechanism.

The CFD code Fluent 22.0 [14] is used to solve the governing equations of energy, mass conservation, momentum and chemical species in the fluid, using a second-order upwind scheme. Coupled algorithm, which is a pressure-velocity coupling method, is used in the simulation. The simulation is considered converged when the residuals for all parameters, 10^{-3} for continuity, are lower than 10^{-4}. To check for convergence and residuals, the simulation monitors the midline temperature and the mass fractions of the main combustion products. A three-dimensional steady model is utilized, neglecting the influence of gravity. The fundamental governing equations for heat and mass transfer are provided. A segregated solution solver with a sub-relaxation method is used. The effect of convection and radiation (P1 model) on the heat losses are computed. An ideal gas flow model is adopted with a mixing law Cp. A weighted-sum-of-gray-gases domain-based model is applied to define mixture absorption coefficient. A numerical model is proposed in this study to analyse combustion chemical effects. The combustion mechanism initially proposed by Mei et al.[15] underwent modification and validation. This updated mechanism incorporates the base H2 mechanism from a recent study by Hashemi et al. [16] , along with the NH3 sub-mechanism from Shrestha et al. Additionally, it includes reactions involving excited species, such as O (1 D) and O2 (a1Δg), as introduced by Konnov [18]. The final revised mechanism encompasses a total of 287 reactions and 43 species.

2.3 Validation of numerical kinetic model

To assess the suitability of the reaction mechanisms used in this study, a validation analysis was performed by comparing the experimental and predicted laminar burning speeds. Within the combustion process, laminar flame speed represents a critical feature that underpins many significant flame properties, including stability, extinction, and flashback. Kinetic simulations were carried out using CHEMKIN with different mechanisms to explore the flame propagation limits of NH_3/air and H_2/air mixture [19]. The modelling of laminar burning velocities was accomplished utilizing the premixed laminar flame speed reactor (PLFSR) testing modules. All simulations achieved convergence to a grid-independent solution. The validation of updated NH3/air kinetic mechanism was performed using experimental data testified by Mei et al., where the laminar burning velocities of NH_3/air at several equivalence ratios were correlated, as illustrated in Figure 1a [15]. The present mechanism proves good agreement with experimental data in lean, stoichiometric, and a little rich condition (<1.2). However, minor variations considering rich side are observed, attributable to the low predicted values of laminar burning velocity of NH_3/air mixtures.

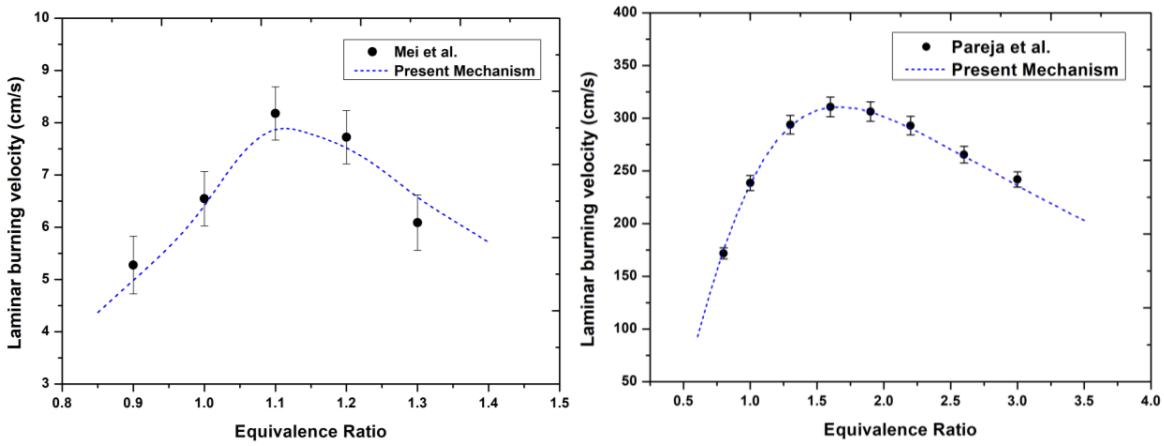

Figure 1. a) LBV of NH_3/air flame, b) LBV of H_2/air flames both at standard conditions

Figure 1 b is showing the LBV of H_2 /air flames at atmospheric temperature (298 K) and pressure (1 atm). In the graph, the symbols signify the experiment data reported by Pareja et al, whereas line shows the findings of the present model. The predicted values of present mechanism exhibit favorable agreement with experimental results [20]. Findings from these studies emphasize that the LBV of ammonia/air reaches its peak at an equivalence ratio (Φ) of approximately 1.1–1.15, while hydrogen/air attains its peak at Φ of around 1.50–1.70, with a laminar burning velocity peak value approximately 40 times higher than that of the NH_3/air combustion.

2.4 Boundary conditions and computational domain

The experimental setup involves employing two distinct channels—one for pure H2 or NH3 and the other for air. Both channels serve as inlet conditions, maintaining constant flow rates and an inlet temperature of 300 K. At the outlet, a pressure-outlet boundary condition of 101325 Pa is set. The wall is characterized as a no-slip surface, incorporating heat transfer to the surroundings. This is modeled through mixed thermal conditions, encompassing a heat transfer coefficient of 20 W/m²-K. The specific quartz glass specific heat capacity and thermal conductivity are 750 J/kg-K and 2 W/m-K [21]. A direct comparison between hydrogen and ammonia as fuels was carried out by establishing a mixture velocity of 6 m/s for hydrogen and varying the equivalence ratio from ignition to 1. For ammonia, mass flow rates were calculated based on different Lower Heating Values (LHV), ensuring an equivalent heat of reaction source (HRS) for each fuel type at the same equivalence ratio. Table 1 reports the inlet velocity magnitude boundary condition for every considered case. Mesh is realized using hexahedral cells, except for the confluence zone, where

prismatic cells are used (Figure 2 a). Additionally, a further refinement of the mesh is applied for the microcombustor inlet region, where the two duct of fuel and air became one single duct regions.
To assurance the grid independence, the simulation results were compared (v=6 m/s, H_2/air case Φ =1) with three difference grid resolutions (140k, 175k and 237k cells). The process of calculating the Grid Convergence Index (GCI) was carried out for three distinct mesh sizes, as detailed in source [22]. This calculation was instrumental in identifying and quantifying the discretization errors inherent in the numerical simulations, thereby enhancing the precision and dependability of the models. The GCI calculated for the finest mesh was found to be 0.2%, whereas for the coarsest mesh, it was determined to be 0.5%. Additionally, an extrapolated value of f* was determined, indicating a medium mesh error of 0.5%, which falls within the acceptable confidence level of 5%. Figure 2b illustrates the outcomes along the midline of the mixture channel for various mesh refinements, specifically for a velocity of 6 m/s in a H2/air mixture at an equivalence ratio (Φ) of 1.

Table 1. Fuelling conditions

		H_2- air		**NH_3-air**	
Φ	**HRS[W]**	**V_{fuel}[m/s]**	**V_{air} [m/s]**	**V_{fuel}**	**V_{air} [m/s]**
0.5	15.2	1	5		
0.6	17.6	1.16	4.83	0.87	6.06
0.7	19.9	1.31	4.69	0.98	5.81
0.8	22.1	1.46	4.54	1.09	5.67
0.9	24.1	1.59	4.41	1.17	5.49
1	26	1.72	4.28	1.29	5.33

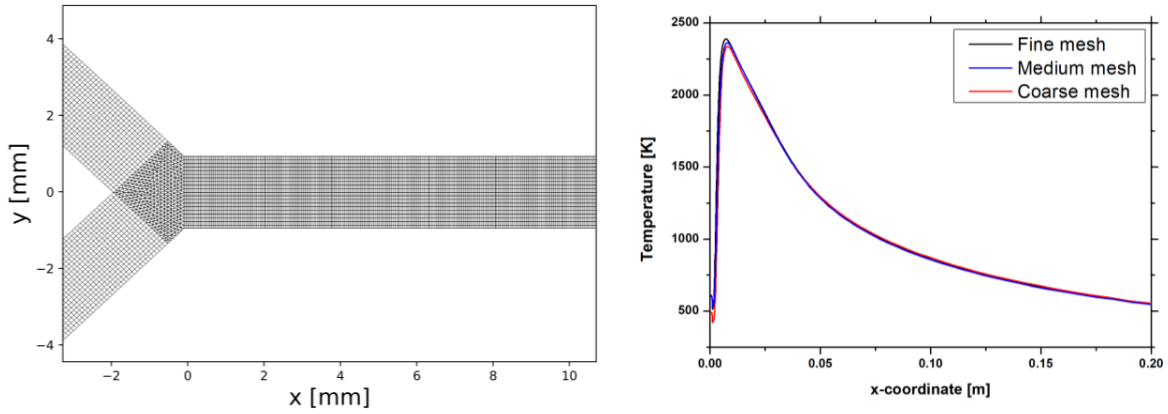

Figure 2. a) Discretization in the mixing zone, b) Grid independent study: midline temperature profile for v=6 m/s, H_2/air case Φ =1.

2.5 Validation of 3D modeling
The simulation results were juxtaposed with experimental observations, focusing on velocity (V) of 6 m/s and spanning equivalence ratios from 0.5 to 1. Notably, for equivalence ratio (Φ) values beneath 0.6, the computational models failed to sustain a stable flame. This instability is consistent with the patterns noted in the corresponding experimental findings [12].
There isn't a straightforward numerical parameter in the simulations that directly corresponds to the chemical flame length for immediate comparison with the observed flame length in experiments. However,

relationships have been identified between the flame characteristics and the mole fraction of OH radicals. It's important to recognize that the chemical flame length is generally more extensive than the visible flame length observed. Furthermore, the intensity of OH fluorescence measured in experiments may not always accurately depict the actual mole fraction of OH radicals.
Despite the limitations, this study identifies a promising correlation between the distribution of the heat of reactions and the flame length. Employing a threshold of $1e^{+9}$ W/m³, meaningful insights can be derived from examining the relationship between the heat of reactions and flame length. Figure 3 depicts the relationship between the reaction heat and flame length, as inferred from photographs of experimental data. Although there are slight variations, like the outlier at an equivalence ratio of 0.9, the general pattern aligns well with the observations from the experiments.

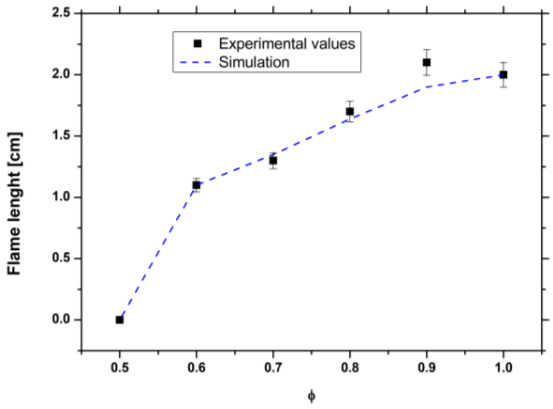

Figure 3. Comparison between experimental and prediction flame length at different equivalence ratios

3 Results

To understand the effects of different fuels and ϕ variations, an investigation was carried out. This involved adjusting ϕ from 0.5 to 1.0, while ensuring the thermal power remained constant for both fuels adhering to the conditions outlined in Table 1. The findings indicated that with hydrogen as the fuel, a flame occurs once the equivalence ratio surpasses 0.5. However, with ammonia, a higher equivalence ratio of at least 0.7 is necessary to initiate a stationary flame. This is due to ammonia lower laminar burning velocity compared to that of hydrogen and other hydrocarbon fuels, which makes maintaining a flame at lower equivalence ratios more difficult. The chemical properties of ammonia also cause the flames to shift towards the outlet, with flame positions for ammonia being noticeably further downstream than those for hydrogen. Simulations focusing on the combustion of ammonia have demonstrated that increasing the fuel-oxidizer equivalence ratio results in reduced NOx emissions, a trend illustrated in Figure 4.

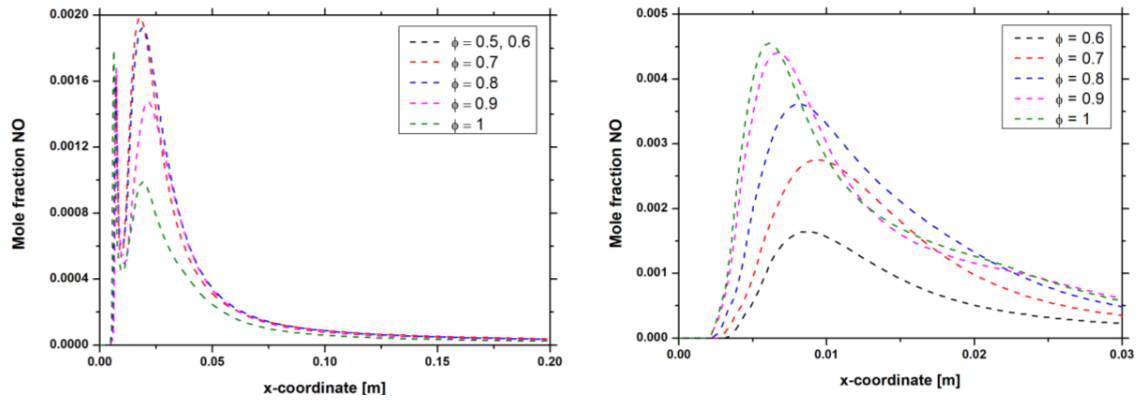

(a) (b)

Figure 4. NO mole fraction midline for a) NH_3/air case and b) H_2/air.

Higher combustion efficiency in ammonia combustion processes at higher equivalence ratios contributes to lower NOx emissions as more of the fuel is completely combusted, with less free oxygen that would lead to NO_x formation. Therefore, optimizing ammonia combustion processes towards richer mixture conditions is advantageous for lowering NOx output. Thermal-NO mechanism is another crucial pathway for NO production, significantly influenced by temperature. This mechanism becomes more pronounced at higher temperatures, leading to an increased formation of NO. Specifically, the concentration of NO measured as the mole fraction in the hydrogen/dry air mixture is found to be twice as high compared to that in the ammonia/air combustion process. This distinction underscores the influence of combustion temperature on NO production rates, highlighting the thermal-NO mechanism role. Radicals such as N_2O, OH, H, and O radicals are crucial to the chemistry of NOx within ammonia flames, primarily through the fuel NOx pathways. In the case of the hydrogen flame, OH mole fraction function shifts upstream proving the different positions of the flame reaction area (Figure 5).

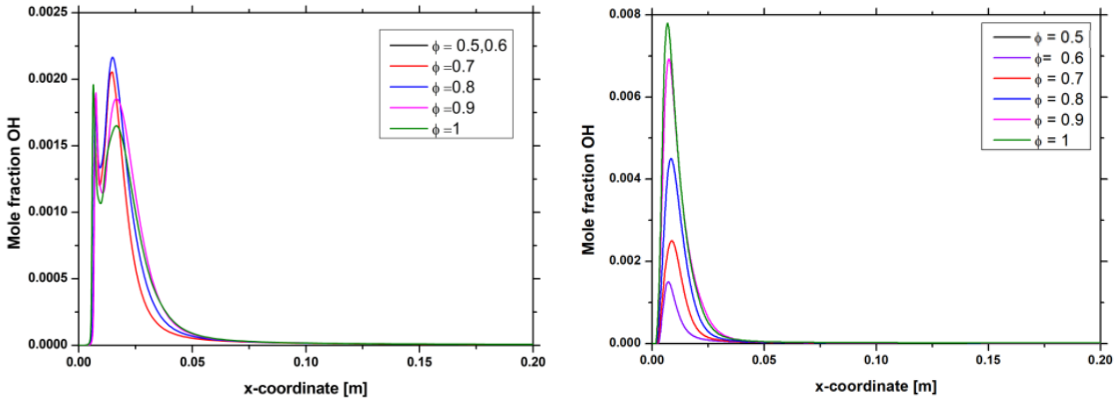

(a) (b)

Figure 5. OH mass for different equivalence ratios for a)NH_3/air case and for b) H_2/air case

Temperature symmetry plane contours at ϕ=0.9 are shown in Figure 6 for both fuel mixtures. The hydrogen flame is observed to stretch into the air side, in contrast, the ammonia flame is displaced towards the outlet, showing a 7 mm downstream shift. This displacement underscores the distinct combustion characteristics and flame stabilization mechanisms between ammonia and hydrogen fuels. Maximum temperature of NH_3/air flames is approximately 200 K lower than that of H_2/air flames.

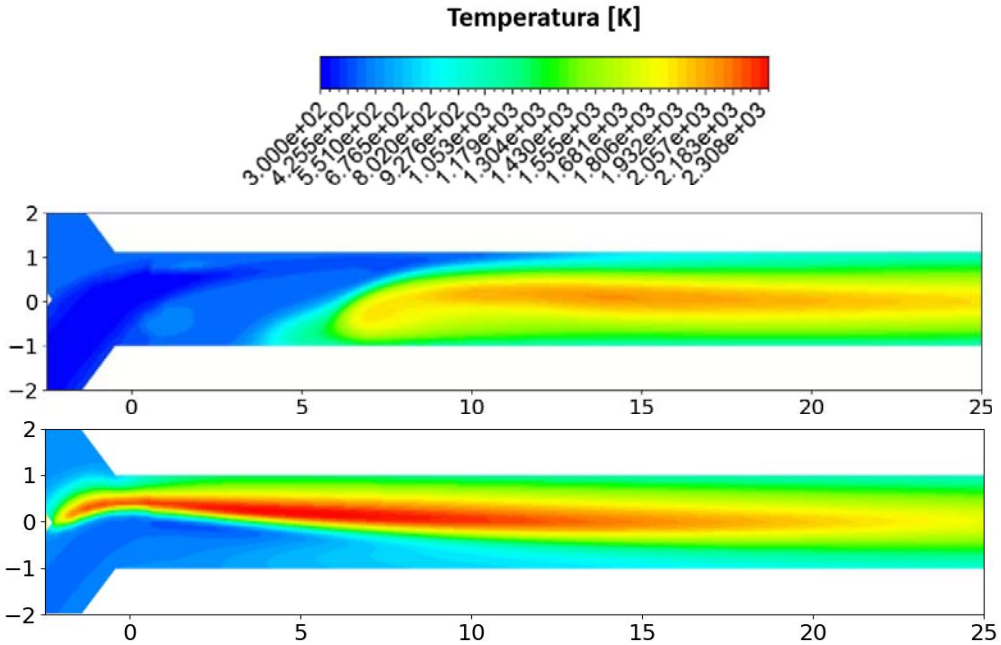

Figure 6. Symmetry plane contours of temperature for fuel power = 24.1 W, Φ=0.9 for NH3/air a) and H2/air condition. Coordinates in mm

4 Conclusion

This study aims to characterize a Y-shaped micro combustor fuelled with green fuels. The unique properties of micro combustors can result in variations in the combustion behaviour of hydrogen and ammonia compared to larger-scale combustion systems. A 3D numerical model integrating detailed kinetic mechanism is developed and validated by relating the predicted values of experimental data found in the literature. The thermal performance and NOx formation mechanism are evaluated in the cases of NH_3/air mixture and H_2/air mixtures for a constant velocity flow of 6 m/s and different Φ.

Results show the effect of the different fuels in terms of produced species, emissions and efficiency of the micro combustor. In case of hydrogen, stable flames can be reached even at low Φ, and the flame temperature is higher with more pollutant production. However, the use of H_2 leads to a rise in the thermal NOx production. The challenge of sustaining a flame at lower equivalence ratios is attributed to the lower LBV of ammonia compared to hydrogen and hydrocarbon fuels. Moreover, for leaner mixtures, the NOx production increase for ammonia cases making the use of hydrogen under lean conditions an even more correct choice**.**

References

[1] Y. Zhang, Q. Lu, B. Fan, L. Long, E. K. Quaye, and J. Pan, ‘Effect of multiple bluff bodies on hydrogen/air combustion characteristics and thermal properties in micro combustor’, *International Journal of Hydrogen Energy*, vol. 48, no. 10, pp. 4064–4072, Feb. 2023, doi: 10.1016/j.ijhydene.2022.10.268.

[2] Y. Yan, C. Zhang, J. Gao, K. Shen, and W. Gao, ‘Numerical study on premixed hydrogen/air combustion characteristics and heat transfer enhancement of micro-combustor embedded with pin fins’, *International Journal of Hydrogen Energy*, vol. 46, no. 77, pp. 38519–38534, Nov. 2021, doi: 10.1016/j.ijhydene.2021.09.097.

[3] W. Zuo *et al.*, 'Effects of injection strategies on thermal performance of a novel micro planar combustor fueled by hydrogen', *International Journal of Hydrogen Energy*, vol. 47, no. 14, pp. 9018–9029, Feb. 2022, doi: 10.1016/j.ijhydene.2021.12.206.
[4] J. Wan and A. Fan, 'Recent progress in flame stabilization technologies for combustion-based micro energy and power systems', *Fuel*, vol. 286, p. 119391, Feb. 2021, doi: 10.1016/j.fuel.2020.119391.
[5] Y. Ju and K. Maruta, 'Microscale combustion: Technology development and fundamental research', *Progress in Energy and Combustion Science*, vol. 37, no. 6, pp. 669–715, Dec. 2011, doi: 10.1016/j.pecs.2011.03.001.
[6] Q. Li, W. Zuo, Y. Zhang, J. Li, and Z. He, 'Effects of rectangular rib on exergy efficiency of a hydrogen-fueled micro combustor', *International Journal of Hydrogen Energy*, vol. 45, no. 16, pp. 10155–10163, Mar. 2020, doi: 10.1016/j.ijhydene.2020.01.221.
[7] N. S. Kaisare and D. G. Vlachos, 'A review on microcombustion: Fundamentals, devices and applications', *Progress in Energy and Combustion Science*, vol. 38, no. 3, pp. 321–359, Jun. 2012, doi: 10.1016/j.pecs.2012.01.001.
[8] J. Chen, L. Yan, W. Song, and D. Xu, 'Effect of heat and mass transfer on the combustion stability in catalytic micro-combustors', *Applied Thermal Engineering*, vol. 131, pp. 750–765, Feb. 2018, doi: 10.1016/j.applthermaleng.2017.12.059.
[9] Q. Peng *et al.*, 'Experimental and numerical investigation of a micro-thermophotovoltaic system with different backward-facing steps and wall thicknesses', *Energy*, vol. 173, pp. 540–547, Apr. 2019, doi: 10.1016/j.energy.2019.02.093.
[10] J. Zhou, Y. Wang, W. Yang, J. Liu, Z. Wang, and K. Cen, 'Combustion of hydrogen–air in catalytic micro-combustors made of different material', *International Journal of Hydrogen Energy*, vol. 34, no. 8, pp. 3535–3545, May 2009, doi: 10.1016/j.ijhydene.2009.01.032.
[11] O. F. Alrebei, L. M. Le Page, G. Mckay, M. H. El-Naas, and A. I. Amhamed, 'Recalibration of carbon-free NH3/H2 fuel blend process: Qatar's roadmap for blue ammonia', *International Journal of Hydrogen Energy*, vol. 48, no. 61, pp. 23716–23736, Jul. 2023, doi: 10.1016/j.ijhydene.2023.03.045.
[12] Y. Xiang, S. Wang, Z. Yuan, and A. Fan, 'Effects of channel length on propagation behaviors of non-premixed H2-air flames in Y-shaped micro combustors', *International Journal of Hydrogen Energy*, vol. 45, no. 39, pp. 20449–20457, Aug. 2020, doi: 10.1016/j.ijhydene.2019.11.147.
[13] Y. Xiang, Z. Yuan, S. Wang, and A. Fan, 'Effects of flow rate and fuel/air ratio on propagation behaviors of diffusion H2/air flames in a micro-combustor', *Energy*, vol. 179, pp. 315–322, Jul. 2019, doi: 10.1016/j.energy.2019.05.052.
[14] 'Ansys | Engineering Simulation Software'. Accessed: Jul. 20, 2023. [Online]. Available: https://www.ansys.com/
[15] Bowen Mei, Jianguo Zhang, Xiaoxiang Shi, Zhongya Xi, Yuyang Li Enhancement of ammonia combustion with partial fuel cracking strategy: 'Laminar flame propagation and kinetic modeling investigation of NH3/H2/N2/air mixtures up to 10 atm' 2021 Combustion and Flame 231 111472 https://doi.org/10.1016/j.combustflame.2021.111472.
[16] H. Hashemi, J. M. Christensen, S. Gersen, and P. Glarborg, 'Hydrogen oxidation at high pressure and intermediate temperatures: Experiments and kinetic modeling', *Proceedings of the Combustion Institute*, vol. 35, no. 1, pp. 553–560, Jan. 2015, doi: 10.1016/j.proci.2014.05.101.
[17] K. P. Shrestha, L. Seidel, T. Zeuch, and F. Mauss, 'Detailed Kinetic Mechanism for the Oxidation of Ammonia Including the Formation and Reduction of Nitrogen Oxides', *Energy Fuels*, vol. 32, no. 10, pp. 10202–10217, Oct. 2018, doi: 10.1021/acs.energyfuels.8b01056.
[18] A. A. Konnov, 'On the role of excited species in hydrogen combustion', *Combustion and Flame*, vol. 162, no. 10, pp. 3755–3772, Oct. 2015, doi: 10.1016/j.combustflame.2015.07.014.
[19] R. J. Kee, F. M. Rupley, and J. A. Miller, 'Chemkin-II: A Fortran chemical kinetics package for the analysis of gas-phase chemical kinetics', Sandia National Lab. (SNL-CA), Livermore, CA (United States), SAND-89-8009, Sep. 1989. doi: 10.2172/5681118.

[20] J. Pareja, H. J. Burbano, and Y. Ogami, 'Measurements of the laminar burning velocity of hydrogen–air premixed flames', *International Journal of Hydrogen Energy*, vol. 35, no. 4, pp. 1812–1818, Feb. 2010, doi: 10.1016/j.ijhydene.2009.12.031.
[21] S. Cai, W. Yang, Y. Ding, Q. Zeng, and J. Wan, 'Hydrogen-air premixed combustion in a novel micro disc-burner with an annular step', *Fuel*, vol. 313, p. 123015, Apr. 2022, doi: 10.1016/j.fuel.2021.123015.
[22] L. E. Schwer, 'IS YOUR MESH REFINED ENOUGH? Estimating Discretization Error using GCI', . *LS*, 2008.